# Determining the Accuracy of Calculating Systolic Wall Thickening Using a Fast Fourier Transform Approximation: A Simulation Study Based on Canine and Patient Data

C. David Cooke, Ernest V. Garcia, S. James Cullom, Tracy L. Faber and Roderic I. Pettigrew

*Division of Nuclear Medicine, Department of Radiology, Emory University School of Medicine, Atlanta, Georgia*

The high count yields of $^{99m}$Tc-sestamibi make possible the acquisition of multiple gated SPECT studies with relatively high count densities. By reorienting these studies into gated short-axis slices, and extracting the three-dimensional myocardial perfusion distribution, we can study wall thickening using an amplitude and phase analysis methodology that examines the change in counts throughout the cardiac cycle. There have been two main concerns raised about this count-based technique: (1) What effect does the sampling rate have on the calculation of systolic wall thickening? and (2) What effect does count density have on the calculation of systolic wall thickening? **Methods:** We designed a simulation study using myocardial wall thickening data obtained from ultrasonic crystals implanted in the myocardium of a normal canine. This data was modified to produce wall thickening curves with various percent systolic wall thickening measurements, sampling rates and count densities. **Results:** The results show that using at least eight frames per cardiac cycle, systolic wall thickening can be calculated with enough accuracy to separate normal patients from those with cardiac dysfunction, even in areas of hypoperfused myocardium. Also, the results show the importance of calculating and interpreting phase (onset of contraction) information. **Conclusions:** This count-based technique continues to show promise as a tool for calculating systolic wall-thickening from multiple gated myocardial perfusion SPECT studies, but needs to be validated in a prospective multi-center trial before being applied in a clinical setting.

**Key Words:** systolic wall thickening; first harmonic analysis; phase and amplitude analysis; technetium-99m myocardial perfusion studies; fast Fourier transform

**J Nucl Med 1994; 35:1185–1192**

With the limited resolution of cardiac SPECT studies, it is not possible to accurately measure the wall thickness of the left-ventricle using geometric methods (*1*). However, it has been shown that the change in myocardial wall thickness is approximately linear to the change in maximum counts extracted from the same myocardial region (*2*), making the measurement of left-ventricular wall thickening a possibility using a multiple gated SPECT acquisition and $^{99m}$Tc-sestamibi myocardial perfusion studies (*3*). Count-based methods of measuring wall thickening have been applied to $^{99m}$Tc-sestamibi-gated planar studies (*4–8*), $^{99m}$Tc-gated SPECT studies (*3*), $^{13}$N-gated PET studies (*9,10*), and $^{201}$Tl-gated SPECT studies (*11*).

We have developed and reported (*12–15*) a count-based method to extract systolic wall-thickening (SWT) from $^{99m}$Tc-sestamibi-gated SPECT studies using eight frames per cardiac cycle, but there have been some questions and concerns raised over both the count-based methodology and the relatively small number of frames per cardiac cycle. To address these concerns, we developed a simulation study based on wall-thickness data obtained from ultrasonic crystals implanted in a normal canine myocardium. This paper will present the results from this simulation study, and address the following questions: (1) What errors are associated with calculating SWT using an eight-frame gated SPECT acquisition?; (2) What errors are associated with calculating SWT using the first harmonic of a fast Fourier transform (FFT) as an approximation of SWT?; and (3) Can SWT be accurately measured in regions of hypoperfused myocardium?

## MATERIALS AND METHODS

### Canine Data

Myocardial wall-thickness data were obtained from a normal canine model, using opposed ultrasonic crystals implanted across the thickness of the myocardium. One cardiac cycle of the wall thickness data was digitized from a strip-chart recording originating at peak left ventricular pressure change (dp/dt, Fig. 1). This curve was digitized using 61 points and linearly interpolated to 64 points. The resulting curve was then shifted such that the beginning of the curve was at the beginning of the R-R interval (Fig. 2). This interpolated canine curve provided a normal wall thickening template with a temporal resolution not achievable with gated SPECT.

Received Nov. 18, 1993; revision accepted Mar. 3, 1994.
For correspondence or reprints contact: C. David Cooke, MSEE, Division of Nuclear Medicine, Emory University Hospital, Atlanta, GA 30322.

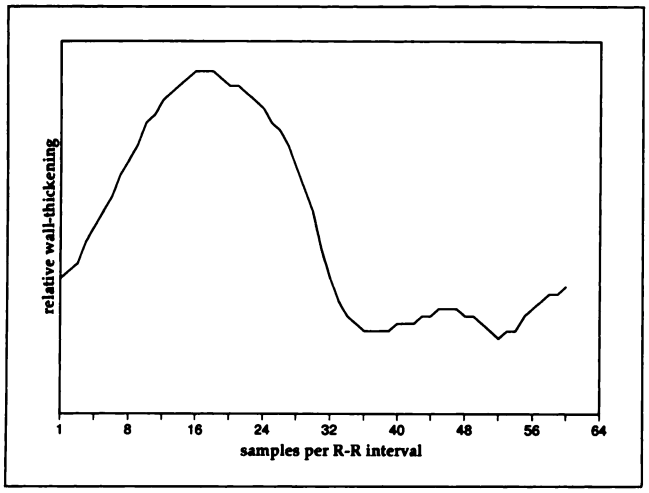


**FIGURE 1.** Original wall-thickening curve, digitized to 61 points from a strip-chart recording.

### Patient Data

Gated myocardial perfusion distributions from 10 normal male volunteers were analyzed to determine the amount of noise and average peak count density present in normal studies. Using this data along with the canine wall thickening template, wall thickening curves representative of normal human studies were created by scaling and shifting the template to reflect the average peak count density found in the male volunteers. These male volunteers had <5% likelihood of coronary artery disease (CAD) and an average age of 47 ± 9 yr, with a range of 35–62 yr. They were imaged using a standard 1-day $^{99m}$Tc-sestamibi clinical protocol, which has been described previously (*16*). This protocol consisted of injecting 8 mCi of $^{99m}$Tc at rest, followed in 3 hr by 22 mCi of $^{99m}$Tc at peak stress and acquiring the images using a high-resolution collimator, 64 × 64 matrix, 64 stops over 180° (25 sec/stop for rest; 20 sec/stop for stress), and ECG gating of the stress study (8 frames/cardiac cycle).

For myocardial perfusion evaluation, all of the gated planar projections were added together as though the study had been acquired nongated, and prefiltered using a Butterworth filter with high-resolution characteristics (cutoff = 0.52 cycles/cm, power factor = 5). A different Butterworth filter, with lower resolution characteristics, was used to pre-filter the multiple gated myocardial perfusion SPECT study (cutoff = 0.4 cycles/cm, power factor = 10). Gated short-axis slices were obtained by reconstructing and reorienting the gated planar projections obtained from the eight-frame gated acquisition.

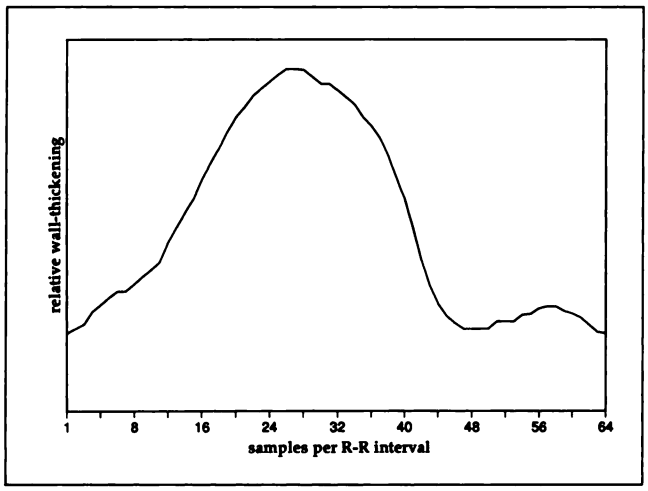


**FIGURE 2.** Original wall-thickening curve, interpolated to 64 points and shifted so that the beginning of the R-R interval was at the origin.

Each of the eight short-axis datasets was reframed using a 2 by 1 methodology, i.e., for each short-axis dataset, slices 1 and 2 were added together to form a new slice 1, slices 2 and 3 were added together to form a new slice 2, etc. Using these reframed datasets, the three-dimensional maximal-count perfusion distribution was extracted using a previously described three-dimensional hybrid sampling scheme that samples the apical portion of the myocardium in spherical coordinates, and the remaining portion of the myocardium in cylindrical coordinates (*16,17*). The average end-systolic maximal counts for the 10 normal male volunteers, for 8 frames/cardiac cycle, was 199 and was used as the standard for normal wall thickening (for simplicity, this will be rounded to 200).

### Simulation Methodology

To assess the errors involved in count-based wall thickening measurements, simulations were done by varying several parameters: (1) number of frames/cardiac cycle; (2) end-systolic count density; (3) systolic wall-thickening percent; and (4) region size.

A simulation consisted of the following steps: (1) sampling the canine wall thickening template to produce a curve of the desired frames/cardiac cycle; (2) scaling and shifting this curve to reflect the desired systolic wall thickening and end-systolic count density; (3) adding random noise; (4) constructing a region of the desired number of pixels; and (5) performing a Fourier analysis on the pixels in the region and calculating an average percent systolic wall thickening for the region.

To produce simulations at different frames/cardiac cycle, the canine wall thickening template of 64 points was summed to produce a curve with the correct number of frames/cardiac cycle and corresponding counts. For instance, to produce a simulation at 8 frames/cardiac cycle, the counts from the first 8 points of the 64-point template were summed together to produce the first point, the counts from the second 8 points were summed together to produce the second point, continuing on, resulting in a curve of 8 points. Using a predetermined end-systolic count density (selected as a percentage of the average end-systolic counts in the normal male patients) and % SWT, the end-systolic counts (ESC) and end-diastolic counts (EDC) were calculated from the following formulas:

$$ESC = 200n, \qquad \text{Eq. 1}$$

$$EDC = \frac{ESC}{\left(1 + \frac{SWT}{100}\right)}, \qquad \text{Eq. 2}$$

where n is the percentage of the average ESC from the normal volunteers.

The interpolated curve (corrected for the desired number of frames/cardiac cycle) was then scaled and shifted such that the end-systolic and end-diastolic counts were equal to those calculated using the formulas above. Gaussian-distributed, count-dependent noise was then added to each point in the curve. This

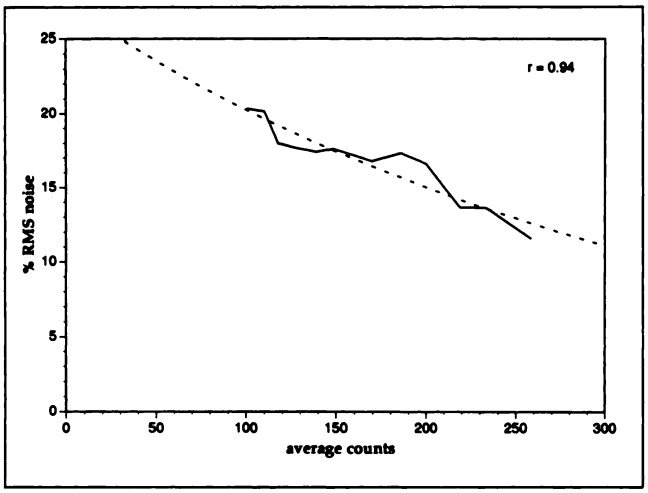


**FIGURE 3.** Percent RMS noise measured in the scans of the 10 normal male volunteers (solid line). An exponential fit of this data is shown in the dashed line.

noise was based on that measured from the gated three-dimensional myocardial perfusion distributions extracted from the short-axis slices of the 10 normal male volunteers. Excluding the first three apical maximal count profiles and the last three basal maximal count profiles, percent error (noise) was calculated as the standard deviation of the maximal counts remaining in the sampled myocardial pixels divided by the average counts in those pixels, for each gate of each normal volunteer. There were a total of 80 points (10 normals × 8 gates/normal), which were grouped into 13 groups of similar count-densities, with statistics performed on these groups. Figure 3 shows average counts from each of these 13 groups plotted against percent RMS noise. An exponential fit was applied to these groups, which yielded the following equation:

$$\% \text{ RMS} = 27.35e^{-0.003cts}, \qquad \text{Eq. 3}$$

where % RMS is the % root mean square error and cts is the counts of the pixel before noise has been added.

Using Equation 3, noise was added to each point in the curve by the following formulas:

$$\sigma = \frac{\% \text{ RMS} \times \text{cts}}{100\%}, \qquad \text{Eq. 4}$$

$$\text{cwn} = g\sigma + \text{cts}, \qquad \text{Eq. 5}$$

where $\sigma$ is the standard deviation of the RMS error; g is a Gaussian-distributed random number with a mean of 0 and a standard deviation of 1; and cwn is the counts of the same pixel after noise has been added.

To simulate the filtering that takes place in the clinical study, nine curves were created using the above techniques and placed into a [3 × 3 × no. of frames/cardiac cycle] data volume. For instance, at 8 frames/cardiac cycle this data volume would consist of 8 frames, with each frame containing nine pixels (arranged in a 3 × 3 matrix) and corresponding to one-eighth of the cardiac cycle. Each frame in this data volume was then spatially smoothed using the following 3 × 3 lowpass filter kernel:

$$\begin{bmatrix} 1 & 2 & 1 \\ 2 & 4 & 2 \\ 1 & 2 & 1 \end{bmatrix}.$$

The regional myocardial count variation throughout the cardiac cycle was created by extracting the center curve out of the above filtered data volume for each pixel in the region. For example, if a region of 10 pixels was desired, then 10 data volumes would be created and the center curve from each filtered data volume would be extracted to form the 10-pixel region.

Once the region was constructed, a one-dimensional FFT was calculated for each pixel in the region. The technique of applying the FFT to extract amplitude and phase information from gated cardiac studies to assess myocardial kinematics was first proposed by Adam et al. (*18*) and further described by Links et al. (*19*). We have applied this technique to assess SWT using the amplitude (amp) of the first harmonic, and the DC component as follows (Fig. 4):

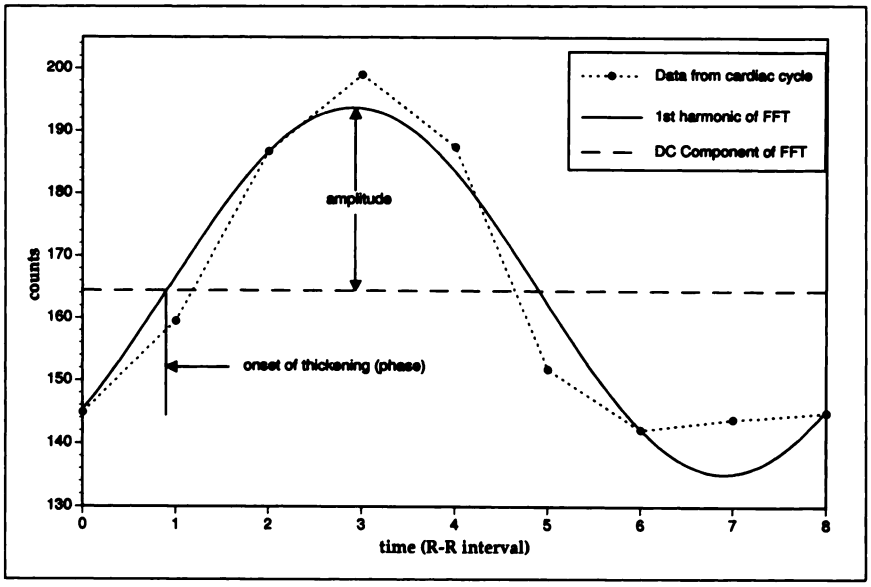


**FIGURE 4.** Graph showing the wall-thickening data down-sampled to eight samples (dotted line with markers). The first harmonic of the corresponding FFT is also shown (solid line), along with the DC component of the FFT (dashed line). Twice the amplitude of the first harmonic of the FFT is used as an approximation of an index proportional to wall thickening. The phase shift of the first harmonic is used as the onset of contraction.

**TABLE 1**
Simulation Parameters Varied to Generate 750 Different Cases

| No. of pixels in region | End-systolic counts (%) | SWT (%) | Frames per cardiac cycle |
|---|---|---|---|
| 5 | 5% | 0.01% | 4 |
| 10 | 10% | 1% | 8 |
| 25 | 25% | 5% | 16 |
| 50 | 50% | 10% | 32 |
| 75 | 100% | 20% | 64 |
| | | 40% | |

$$\% \text{ SWT} = \frac{2\text{amp}}{(\text{DC} - \text{amp})} \times 100\%. \quad \text{Eq. 6}$$

This equation is equivalent to:

$$\% \text{ SWT} = \frac{\text{ESC} - \text{EDC}}{\text{EDC}} \times 100\%. \quad \text{Eq. 7}$$

Phase (onset of contraction) was calculated as the phase shift of the first harmonic of the FFT, also shown in Figure 4.

After the SWT and phase were determined for each pixel in the region, an average SWT and phase were calculated for the entire region. This average region calculation was then repeated 100 times to get an overall average and standard deviation for both phase and SWT (random noise was the only difference between repetitions). This overall average and standard deviation represents the expected spread of results if the same patient had been imaged 100 times.

There were a total of 75,000 simulations done. This consisted of 750 different cases, where each case was run 100 times and averaged as described above. The parameters that were varied to generate the 750 cases are shown in Table 1. Because of space limitations, we will only report the results from a subset of 135 cases (out of the 750) that are more likely to be of use in a clinical setting, or that show a trend in the data. This subset of cases consisted of: (1) sampling rates of 8, 16 and 32 frames/cardiac cycle, since most institutions have the ability to acquire 8 and 16 frames/cardiac cycle; 32 frames/cardiac cycle was included to represent the "best" we could hope for with current technology; (2) region sizes of 5, 25 and 75 pixels, representing approximately 1/120, 1/24, and 1/8 of the myocardium, respectively (Fig. 5); (3) count densities of 10, 50 and 200 counts/pixel (this is equivalent to 5%, 25% and 100% of the average peak end-systolic count density, at 8 frames/cardiac cycle, of the 10 normal male volunteers), which was adjusted for the sampling rate, i.e., 200 counts/pixel at 8 frames/cardiac cycle is equal to 50 counts/pixel at 32 frames/cardiac cycle; and (4) actual SWT of 0% (0.01% was used to approximate 0%, to avoid math overflow errors), 10%, 20% and 40%. The SWT percentages were chosen based on an average myocardial wall thickness of 10 mm, therefore 40% SWT results in 4 mm of thickening, which is considered to be normal (*20*); 20% SWT results in 2 mm of thickening, which is considered to be abnormal; 10% SWT results in 1 mm of thickening, which is considered to be grossly abnormal; and 0% SWT was included to see what effect noise had on the count-based method. These selected parameters are described in the following section.

## RESULTS

Figure 6 shows the results of calculating count-based SWT using the selected parameters described above. Each bar represents the average SWT over 100 separate runs, where the corresponding error bar represents one standard deviation of the SWT over the 100 runs. For instance, the case of 8 frames/cardiac cycle with 5-pixel regions at 40% SWT and 10 counts/pixel had a simulated average % SWT of 47 ± 7 over 100 separate runs. A general trend can be seen in that higher count densities and sampling at greater frames/cardiac cycle yield calculated SWT values that are closer to the actual SWT values. Notice that as actual SWT decreases, there are greater differences between calculated SWT at the different count densities (this is especially evident at 8 frames/cardiac cycle). Notice also that the main difference region size makes at a particular sampling rate is widening of the error bars as the region size gets smaller.

Figure 7 shows five histograms of phases calculated at 8 frames/cardiac cycle, 200 counts/pixel, and over 40%, 20%, 10%, 0%, and −10% (paradoxical thickening or thinning) SWT. Each of the histograms was produced by computing 10,000 separate runs for each SWT and creating a histogram of the resulting phases (10,000 runs were used to reduce variations that can occur when only a few runs are done). The "correct" phase was assumed to be the peak of the 40% SWT histogram, found to be 132°. The two lines on either side of this peak represent ±90°, which is assumed to include all of the phases associated with positive wall thickening. The percent of positive phases gives the percent of the 10,000 phases that fall within this positive wall-thickening region. Notice how the peak spreads out as SWT is decreased. Nevertheless, even at 10% SWT, 95% of the phases are still associated with positive thickening, as opposed to 0% SWT, where the phases are randomly distributed with half of the phases associated with positive thickening and half with negative thickening. Also notice that at −10% SWT, which is actually wall thinning, only 2.4% of the phases fell within the positive wall-thickening region.

Figure 8 shows the percent of positive phases (described in Fig. 7) for all of the selected parameters. The peak phase and ±90° limits were found for each sampling rate by computing a phase histogram for 10,000 runs at each sampling rate at 40% SWT, 200 (or equivalent) counts/pixel. The peak phases were found to be: 132° at 8 frames/cardiac cycle, 142° at 16 frames/cardiac cycle and 148.5° at 32 frames/cardiac cycle. Notice that in contrast to Figure 6, count density has less of an effect on the percent of positive phases and that smaller regions and decreased SWT result in increasing the standard deviation associated with the percent of positive phases. Not shown in this figure are the results from 10 pixel regions. Table 2 shows the average percent of positive phases and standard deviations associated with these percentages for 10 pixel regions, and 8

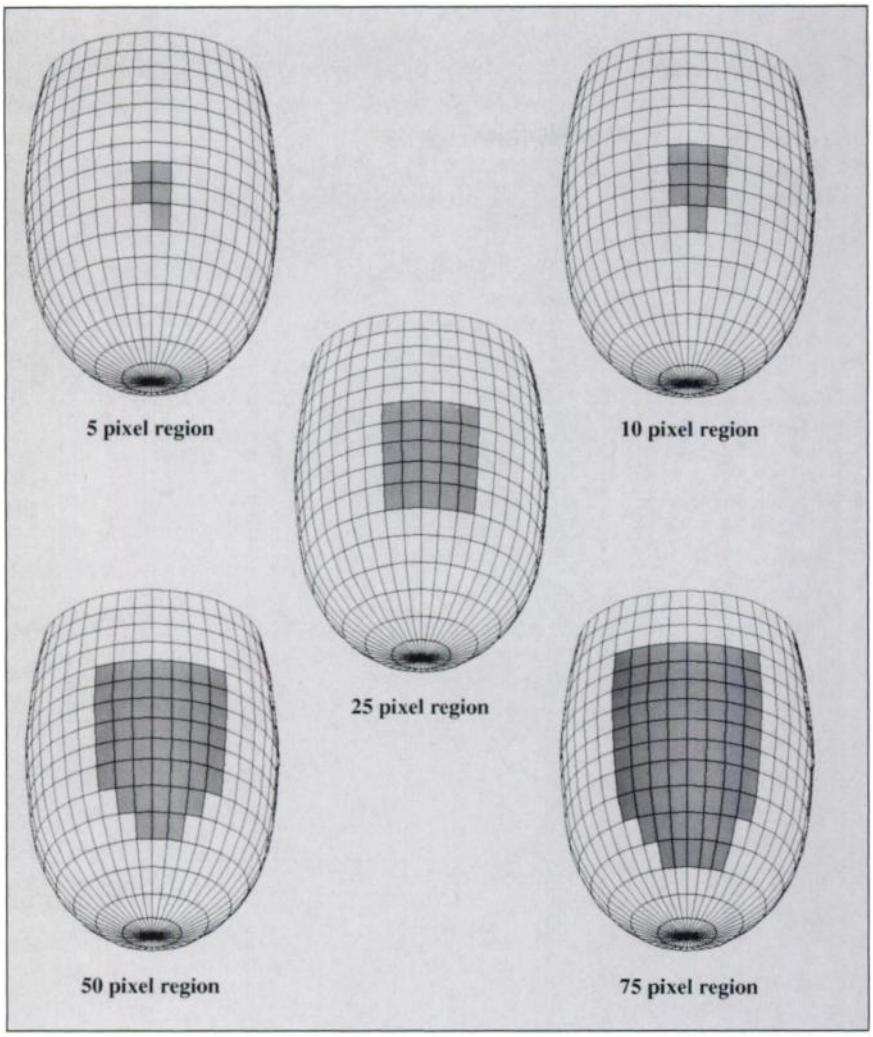


**FIGURE 5.** Comparison of myocardial surface region size (shown in gray) for determining wall thickening.

frames/cardiac cycle. These averages were calculated across three different count densities (200, 50 and 10 counts/pixel).

## DISCUSSION

The simulation described above was designed to study the limitations and errors involved in calculating SWT and the onset of SWT (phase) using a count-based method. In particular, we wanted to address three questions: (1) What errors are involved in acquiring 8 frames/cardiac cycle? (2) What errors are involved in using the first harmonic of the FFT; and (3) Can a count-based method accurately detect SWT in hypoperfused myocardium?

The results presented above demonstrate that the modeled errors associated in acquiring 8 frames/cardiac cycle and calculating SWT using the first harmonic of the FFT are small enough to allow separation of patients with cardiac dysfunction from normals. Even in areas of hypoperfused myocardium, SWT may be accurately determined if the distribution of phases is interpreted properly. This was demonstrated in Figures 7 and 8 and Table 2, which showed how the percent of positive phases varied with SWT. Therefore, to determine if a calculated SWT is accurate, the phases of the region surrounding the point in question must be examined. The size of the region should be greater than five pixels, with better results obtained by using larger regions.

These simulations suggest that if the surrounding region has a Gaussian distribution with the majority (>75%) of the phases within the "positive" region, then the SWT measurement can be assumed to be accurate. If the surrounding region has a random, uniform distribution with only 50% ± 15% of the phases within the positive region, then the SWT measurement should be assumed to be due to noise, and indicative of absent SWT. Lastly, if the surrounding region has a Gaussian distribution with 20% or less of the phases within the positive region, then the SWT measurement can be assumed to be accurately representing wall thinning (negative SWT) rather than wall thickening.

Our results shown in Figure 7, which describe how the phase distribution broadens as SWT decreases, are consistent with those obtained from Schwaiger et al. (*21*) who correlated ejection fraction with phase analysis of radionuclide ventriculograms. Their results showed that as left ventricular function decreased, the standard deviation of

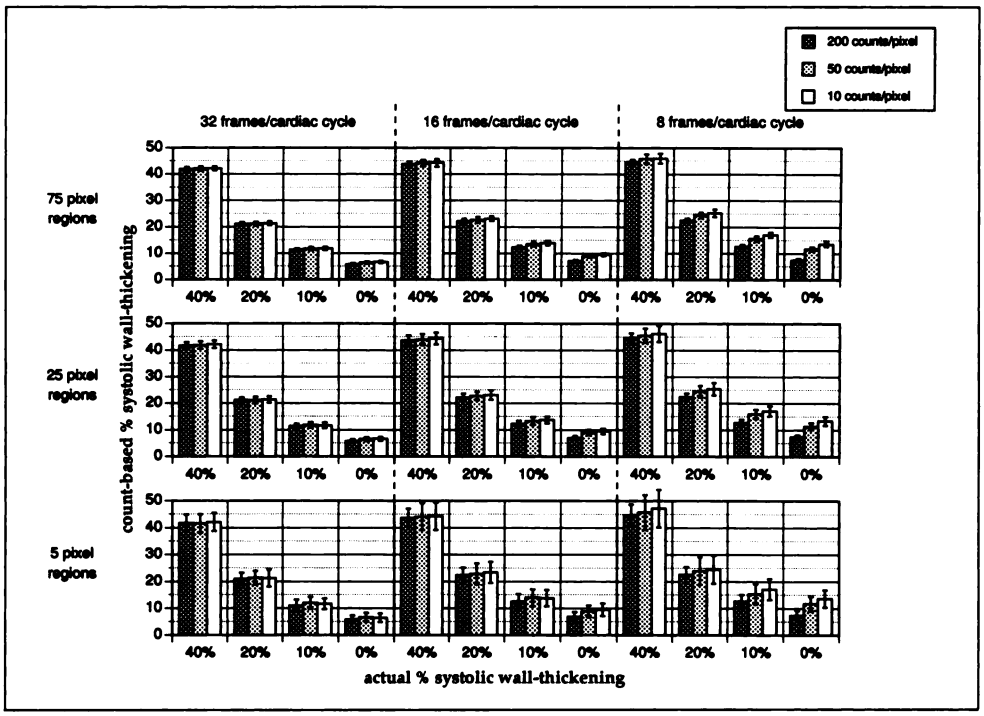


**FIGURE 6.** Count-based % systolic wall thickening and standard deviation (error bars) shown as a function of frames/cardiac cycle, region size and actual % systolic wall thickening. The error bars represent one standard deviation of each parameter calculated from performing 100 consecutive runs with random noise added to each run. Count density refers to eight frames/cardiac cycle. Count densities for other frame rates were scaled appropriately.

the phase distribution increased. This increase in standard deviation was seen in patients with and without CAD and was attributed to the amount of statistical noise present when the activity in the LV is low, or when the amplitude of activity changes is small.

Several investigators have validated a count-based method of calculating SWT as a measure of left ventricular function, similar to the method we described in this paper. Although our simulation was of gated myocardial perfusion SPECT data, these investigators varied in their imaging technique or their assessment of myocardial function. Kahn et al. (*3*), using $^{99m}$Tc-gated SPECT, found that semiquantitative assessment of SWT correctly identified 29/31 reversible perfusion defects. Technetium-99m-gated planar studies have been used by Marcassa et al. (*4*) to show that count-based SWT, measured in 10 normal volunteers, correlated very well with geometric methods applied to both cine CT and MRI.

Marzullo et al. (*7*) showed good agreement (88%) between count-based SWT and wall motion measured by contrast ventriculography. Pace et al. (*8*) demonstrated that count-based SWT improved in 6/6 patients who underwent angioplasty. Nitrogen-13-gated PET studies have been used by Yamashita et al. (*9*) to show that in five normal males, count-based SWT correlated well with that calculated from MRI (r = 0.84) and in 16 male patients with CAD, count-based SWT agreed well with wall motion assessed with conventional left ventriculography. This group has also shown that in 26 male patients with CAD, count-based SWT correlated well with stress-induced ischemia and FDG accumulation.

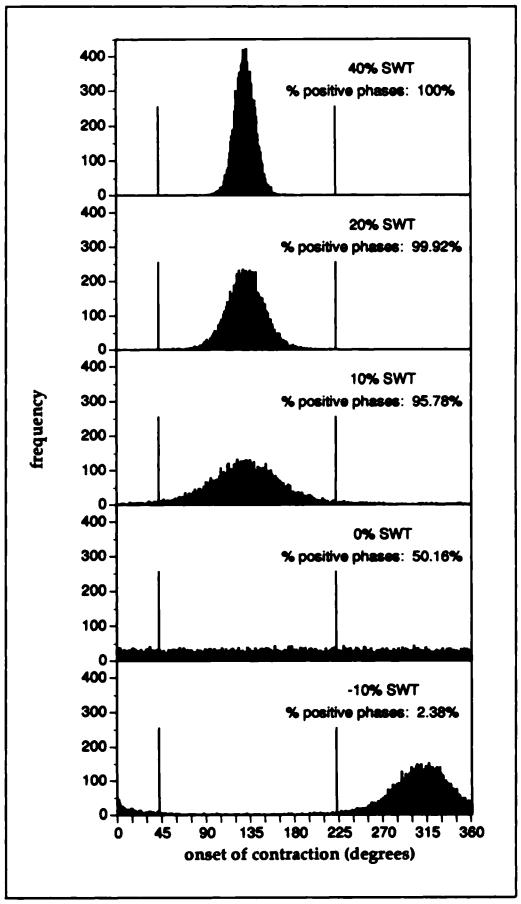


**FIGURE 7.** Histograms of phase of the onset of contraction as a function of % SWT.

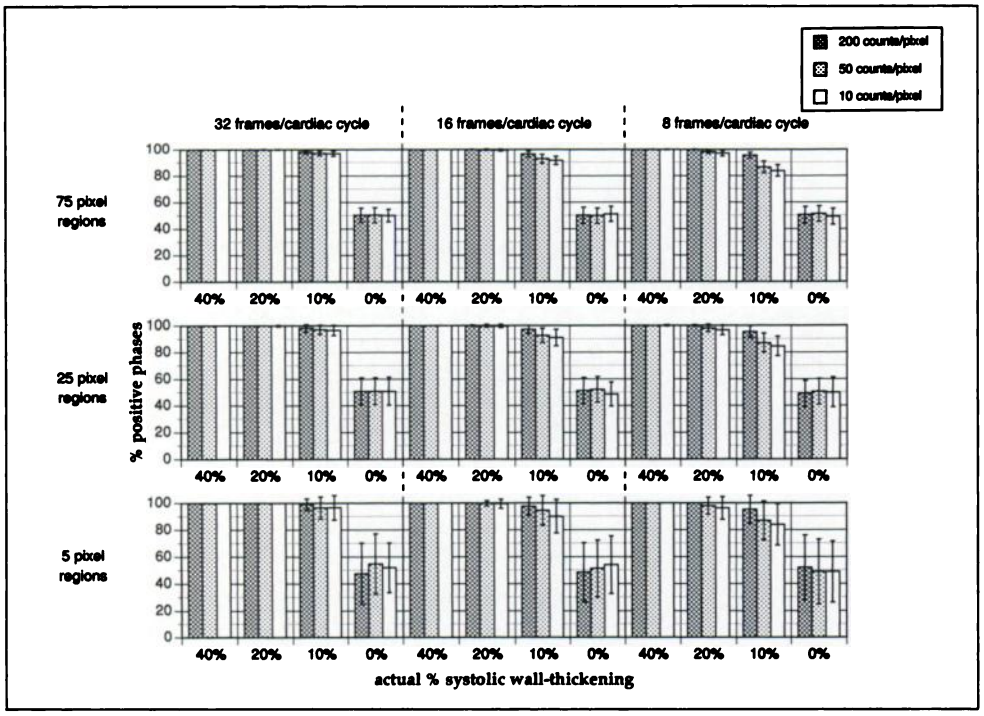


**FIGURE 8.** Percent positive phases of the onset of contraction and standard deviation (error bars) as a function of frames/cardiac cycle, region size and actual % SWT. The error bars represent one standard deviation of each parameter, calculated from performing 100 consecutive runs with random noise added to each run. Count density refers to eight frames/cardiac cycle. Count densities for other frame rates were appropriately scaled.

### Limitations of this Study

Some limitations of this study should be noted. This simulation was accomplished using data from a single normal dog and needs clinical validation in a prospective multicenter trial where the in vivo effects of three-dimensional cardiac motion, partial volume elements, cardiac cycle variable attenuation and variable functional states can be included. Also, we chose to investigate 8 frames/cardiac cycle for several reasons: (1) most nuclear medicine computers can acquire an 8-frame gated SPECT study; (2) there is a significant reduction in storage needs and reconstruction time when only 8 frames are acquired; and (3) the count density (counts/pixel) is greater when 8 frames are acquired (versus 16 or 32) over an average acquisition time of approximately 30 min (the average acquisition time of most myocardial perfusion SPECT protocols).

Importantly, the accuracy of the results obtained is predicated on the observation that a change in wall thickness is directly proportional to a change in counts throughout the cardiac cycle (*2*). This proportionality is better maintained when imaging with a spatial resolution which is low compared to myocardial wall thickness (i.e., wall thickness less than twice the resolution). This proportionality is also better maintained when measuring SWT in regions of the myocardium which are relatively uniform and do not exhibit significant shape distortions as might occur with infarction. The additional error in %SWT associated when imaging with higher resolution or when imaging a distorted myocardial wall has not been included in our calculations but is the topic of other reports (*22,23*).

**TABLE 2**
Average Percent of Positive Phases with Standard Deviations for a Ten-Pixel Region at Eight Frames/Cardiac Cycle for Various SWT Measurements

| Percent SWT | Average Percent of Positive Phases |
|---|---|
| 40% SWT | 100.0 ± 0.0 |
| 20% SWT | 98.3 ± 4.1 |
| 10% SWT | 88.5 ± 11.3 |
| 0% SWT | 50.9 ± 15.0 |
| −10% SWT | 9.7 ± 11.2 |

## CONCLUSIONS

This simulation suggests that multiplegated SPECT studies can be routinely acquired with an adequate number of frames/cardiac cycle to accurately measure SWT using a count-based technique. Our results show that even at 8 frames/cardiac cycle, and in simulated hypoperfused myocardium when phase information is taken into account, the measurement of SWT should be accurate enough to identify patients with cardiac dysfunction. These are encouraging results, but must be interpreted cautiously, as this simulation was performed on animal data and should be validated in a prospective, multicenter trial before being applied in the clinical setting. This count-based technique continues to show promise as a clinical tool, and could potentially allow clinicians to assess both myocardial perfusion and function from a single SPECT study.

## ACKNOWLEDGMENTS

This research was supported in part by National Institutes of Health Grants R01 HL42052 and R01 HL42021 and the E.I. Du Pont De Nemours and Company.

## REFERENCES

1. Eisner RL, Boyers AS, Dunn D, Patterson RE. Inherent limitations in LV wall thickness and mass measurements from SPECT myocardial perfusion scans [Abstract]. *J Nucl Med* 1989;30:796.
2. Galt JR, Garcia EV, Robbins WL. Effects of myocardial wall thickness on SPECT quantification. *IEEE Trans Med Imag* 1990;9:144–150.
3. Kahn JK, Henderson EB, Akers AS, et al. Prediction of reversibility of perfusion defects with a single post-exercise technetium-99m RP-30A gated tomographic image: the role of residual systolic thickening [Abstract]. *J Am Coll Cardiol* 1988;11:31A.
4. Marcassa C, Marzullo P, Parodi O, Sambuceti G, L'Abbate A. A new method for noninvasive quantitation of segmental myocardial wall thickening using $^{99m}$Tc-2-methoxy-isobutyl-isonitrile scintigraphy: results in normal subjects. *J Nucl Med* 1990;31:173–177.
5. Marcassa C, Marzullo P, Sambuceti G, Parodi O. Evaluation of regional myocardial systolic and diastolic function using ECG-gated sestamibi scintigraphy. *Intl J Cardiol Imag* 1993;9:49–55.
6. Marcassa C, Marzullo P, Sambuceti G, Parodi O. Prediction of reversible perfusion defects by quantitative analysis of postexercise electrocardiogram-gated acquisition of $^{99m}$Tc-2-methoxyisobutylisonitrile myocardial perfusion scintigraphy. *Eur J Nucl Med* 1992;19:796–799.
7. Marzullo P, Marcassa C, Sambuceti G, Parodi O, L'Abbate A. The clinical usefulness of electrocardiogram-gated $^{99m}$Tc-methoxy-isobutyl-isonitrile images in the detection of basal wall motion abnormalities and reversibility of stress induced perfusion defects. *Intl J Card Imag* 1992;8:131–141.
8. Pace L, Betocchi S, Piscione F, Mangoni di Santo Stefano ML, Chiariello M, Salvatore M. Evaluation of myocardial perfusion and function by $^{99m}$Tc-methoxy isobutyl isonitrile before and after percutaneous transluminal coronary angioplasty: preliminary results. *Clin Nucl Med* 1993;18:286–290.
9. Yamashita K, Tamaki N, Yonekura Y, et al. Quantitative analysis of regional wall motion by gated myocardial positron emission tomography: validation and comparison with left ventriculography. *J Nucl Med* 1989;30: 1775–1786.
10. Yamashita K, Tamaki N, Yonekura Y, et al. Regional wall thickening of left ventricle evaluated by gated positron emission tomography in relation to myocardial perfusion and glucose metabolism. *J Nucl Med* 1991;32:679–685.
11. Mochizuki T, Murase K, Fujiwara Y, Tanada S, Hamamoto K, Tauxe WN. Assessment of systolic thickening with $^{201}$Tl ECG-gated single-photon emission computed tomography: a parameter for local left ventricular function. *J Nucl Med* 1991;32:1496–1500.
12. Cooke CD, Ziffer JA, Folks RD, Garcia EV. A count-based method for quantifying myocardial thickening from SPECT $^{99m}$Tc-sestamibi studies: description of the method [Abstract]. *J Nucl Med* 1991;32:1068.
13. Cooke CD, Garcia EV, Cullom SJ, Faber TL, Pettigrew RI. Technetium-99m-sestamibi myocardial multiple-gated SPECT simulation for determining the accuracy of count-based systolic wall-thickening measurement [Abstract]. *J Nucl Med* 1993;34:96P.
14. Cooke CD, Garcia EV, Folks RD, Ziffer JA. Myocardial thickening and phase analysis from $^{99m}$Tc-sestamibi multiple gated SPECT: development of normal limits [Abstract]. *J Nucl Med* 1992;33:926.
15. Ziffer JA, Cooke CD, Folks RD, La Pidus AS, Alazraki NP, Garcia EV. Quantitative myocardial thickening assessed with sestamibi: clinical evaluation of a count-based method [Abstract]. *J Nucl Med* 1991;32:1006.
16. Garcia EV, Cooke CD, Van Train K, et al. Technical aspects of myocardial SPECT imaging with $^{99m}$Tc-sestamibi. *Am J Cardiol* 1990;66:23E–31E.
17. Cooke CD, Garcia EV, Folks RD, Peifer JW, Ezquerra NF. Visualization of cardiovascular nuclear medicine tomographic perfusion studies. In: *Proceedings of the First Conference on Visualization in Biomedical Computing*. Atlanta: IEEE Computer Society Press; 1990:185–
18. Adam WE, Tarkowska A, Bitter F, Stauch M, Geffers H. Equilibrium (gated) radionuclide ventriculography. *Cardiovasc Radiol* 1979;2:161–173.189.
19. Links JM, Douglass KH, Wagner HN. Patterns of ventricular emptying by fourier analysis of gated blood-pool studies. *J Nucl Med* 1980;21:978–982.
20. Pflugfelder PW, Sechtem UP, White RD, Higgins CB. Quantification of regional myocardial function by rapid cine MRI. *Am J Roentgenol* 1988; 150:523–529.
21. Schwaiger M, Ratib O, Henze E, Schelbert HR. Limitations of quantitative phase analysis of radionuclide angiograms for detecting coronary artery disease in patients with impaired left ventricular function. *Am Heart J* 1984;108:942–949.
22. Mok DY, Bartlett ML, Bacharach SL, et al. Can partial volume effects be used to measure myocardial thickness and thickening? In: *Computers in cardiology*. Atlanta: IEEE Computer Society Press; 1992:195–198.
23. Bacharach SL, Bartlett M, Vaquero JJ, Mok DY, Dilsizian V. Myocardial thickness by gated PET and SPECT: variability and bias [Abstract]. *J Nucl Med* 1993;34:178P.